Biochemical and Biophysical Research Communications 438 (2013) 452–456

Contents lists available at ScienceDirect

Biochemical and Biophysical Research Communications

journal homepage: www.elsevier.com/locate/ybbrc

A peroxisome biogenesis deficiency prevents the binding of alpha-synuclein to lipid droplets in lipid-loaded yeast

Shaoxiao Wang [a], Patrick J. Horn [b], Liang-Chun Liou [c], Martin I. Muggeridge [d], Zhaojie Zhang [c], Kent D. Chapman [b], Stephan N. Witt [a,*]

[a] Department of Biochemistry and Molecular Biology, Louisiana State University Health Sciences Center, Shreveport, LA 71130, USA
[b] Department of Biological Sciences, Center for Plant Lipid Research, University of North Texas, Denton, TX 76203, USA
[c] Department of Zoology and Physiology, University of Wyoming, Laramie, WY 82071, USA
[d] Department of Microbiology and Immunology, Center for Molecular and Tumor Virology and the Feist-Weiller Cancer Center, Louisiana State University Health Sciences Center, Shreveport, LA 71130, USA

ARTICLE INFO

Article history:
Received 27 June 2013
Available online 31 July 2013

Keywords:
Alpha-synuclein
Lipid droplets
Peroxisome
Parkinson's disease

ABSTRACT

Using a yeast model of Parkinson's disease, we found that alpha-synuclein (αS) binds to lipid droplets in lipid-loaded, wild-type yeast cells but not to lipid droplets in lipid-loaded, peroxisome-deficient cells (*pex3Δ*). Our analysis revealed that *pex3Δ* cells have both fewer lipid droplets and smaller lipid droplets than wild-type cells, and that the acyl chains of the phospholipids on the surface of the lipid droplets from *pex3Δ* cells are on average shorter (C_{16}) than those (C_{18}) on the surface of lipid droplets from wild-type cells. We propose that the shift to shorter ($C_{18} \rightarrow C_{16}$) acyl chains contributes to the reduced binding of αS to lipid droplets in *pex3Δ* cells.

1. Introduction

Alpha-synuclein (αS) is a presynaptic protein that has been linked to Parkinson's disease (PD) [1,2]. αS is thought to be a chaperone that helps catalyze the fusion of neurotransmitter vesicles with the presynaptic membrane [3]. A persistent increased level of αS due to multiplication of the αS locus [4], posttranslational modifications [5], or mutations [6–8] triggers this protein to self-associate into a plethora of high molecular mass soluble and insoluble species, some of which are toxic and capable of spreading pathology from cell to cell [9].

αS binds to vesicles and membranes [10] and even lipid droplets [11]. The rules that govern the binding of αS to these structures have not been completely elucidated. Several groups [12–14] have demonstrated that αS senses membrane curvature and particularly binds to vesicles of high curvature or small diameter, such as presynaptic vesicles (diameter ~50 nm). Here, using a yeast model of PD, we report that αS binds to lipid droplets in lipid-loaded, wild-type cells, whereas it fails to bind to lipid droplets in a lipid-loaded, peroxisome-deficient mutant (*pex3Δ*), which is similar to human Zellweger cells [15]. A lipid droplet has an inner core of neutral lipids and an outer monolayer of phospholipids. Determining the morphological and compositional changes in lipid droplets that occur due to the loss of peroxisome function could lead to a deeper understanding of the molecular determinants that govern the binding of αS to cell membranes.

2. Materials and methods

2.1. Strains, media and reagents

The *Saccharomyces cerevisiae* wild-type strain BY4741 was used in this study. Information on strains and plasmids are given in the Supplementary data (Table S1). For induction of lipid droplets and peroxisomes, cells were pre-grown in synthetic complete (SC) medium (0.67% yeast nitrogen base (YNB), 0.2% amino acids dropout mix) without uracil supplemented with 2% sucrose (SC-Ura/Suc) to exponential phase, and then shifted into inducing medium SC-Ura/Oleate (SC-Ura medium supplemented with 0.5% Oleate and 0.2% Tween 40). For microscopy and lipid droplet preparation, the cells were harvested after 24 h induction at 30 °C. All chemicals were purchased from Sigma.

2.2. Lipid droplet isolation

Wild-type and *pex3Δ* cells were pre-grown in SC-sucrose medium (0.67% yeast nitrogen base (YNB), 0.2% amino acids dropout mix and 2% sucrose) to OD_{600} = 1 and then shifted into SC-Ura/Oleate for 24 h. We closely followed the lipid droplet isolation procedure given in [16] (see Supplementary data for details). Cells were

* Corresponding author. Address: Louisiana State University Health Sciences Center, 1501 Kings Hwy., Shreveport, LA 71130, USA. Fax: +1 318 675 5180.
E-mail address: switt1@lsuhsc.edu (S.N. Witt).

0006-291X/$ - see front matter © 2013 Elsevier Inc. All rights reserved.
http://dx.doi.org/10.1016/j.bbrc.2013.07.100

cultured in liquid media with shaking, harvested after 24 h, and then treated with zymolyase to remove the cell wall. The resultant spheroplasts were homogenized and subjected to several centrifugation steps. Lipid droplets were recovered from the top of the gradient, chemically extracted and subjected to lipidomic analysis by mass spectrometry.

2.3. Mass spectrometry

Total lipids from lipid droplet samples were extracted in hot isopropanol (70 °C) with intermittent vortexing followed by addition of $CHCl_3$ and water for monophasic extraction [17]. Samples that were to be analyzed by direct-infusion electrospray ionization mass spectrometry (ESI-MS) analysis were spiked with an internal standard mixture composed of Tri15:0-triacylglycerol (TAG), Tri21:0-TAG, 13:0-cholesteryl ester, 19:0-cholesteryl ester, Di14:0-phosphatidylcholine (PC), Di14:0-phosphatidylethanolamine (PE), and Di14:0-phosphatidic acid (PA). Neutral lipids (e.g., sterols, steryl esters (Stes), TAGs) were fractionated from polar lipids by silica gel column chromatography in hexane: diethyl ether 4:1 by volume (Supelco Discovery DSC-Si 6 ml, 500-mg solid phase extraction cartridges). Polar lipids (mostly phospholipids) were eluted with methanol then columns rinsed with $CHCl_3$ to elute any remaining lipids. Organic solvents were evaporated off under nitrogen, and samples were resuspended in 200 μl methanol/$CHCl_3$, and stored under nitrogen at −20 °C until analysis. For ESI-MS analysis, lipid extracts were diluted in either 1:2 or 1:1 (v/v) chloroform:methanol plus 10 mM ammonium acetate and were infused at flow rates of 5–10 μl/min into an electrospray source (4 kV spray voltage) of a Thermo TSQuantum triple quadrupole mass spectrometer (Thermo Fisher Scientific). Neutral lipids and phospholipid molecular species were identified in precursor-product scans of each class and quantified against internal standards as described [18].

2.4. Microscopy and Western blotting

Details regarding confocal microscopy and statistical analysis of the data may be found in Supplementary data, and details regarding transmission electron and wide-field microscopy [19] and Western blotting [20] were previously published.

3. Results and discussion

We discovered that αS binds to lipid droplets in lipid-loaded, wild-type yeast cells. To identify mutants with enhanced binding of αS to lipid droplets or with no binding at all, selected mutants from the yeast deletion collection were evaluated under lipid loading conditions. Two peroxisome biogenesis mutants (*pex2Δ* and *pex3Δ*) were identified that were noteworthy, and here we focus on *pex3Δ*.

3.1. αS binds to lipid droplets in lipid-loaded, wild-type cells but not in lipid-loaded, pex3Δ cells

To detect the binding of αS to lipid droplets in yeast cells, two strains were engineered to express fluorescently tagged fusions of both αS and Erg6, which is a resident lipid droplet protein [21]. Strain wt-3xGFP-αS, which was constructed from the parental BY4741 strain, contained three integrated copies of GFP-αS (GFP, green fluorescent protein), where each copy was under the control of a fatty acid promoter (P_{FAA2}), and chromosomal *ERG6* was replaced with *ERG6*-mCherry. The Erg6-mCherry fusion protein is referred to below as Erg6-RFP (RFP, red fluorescent protein).

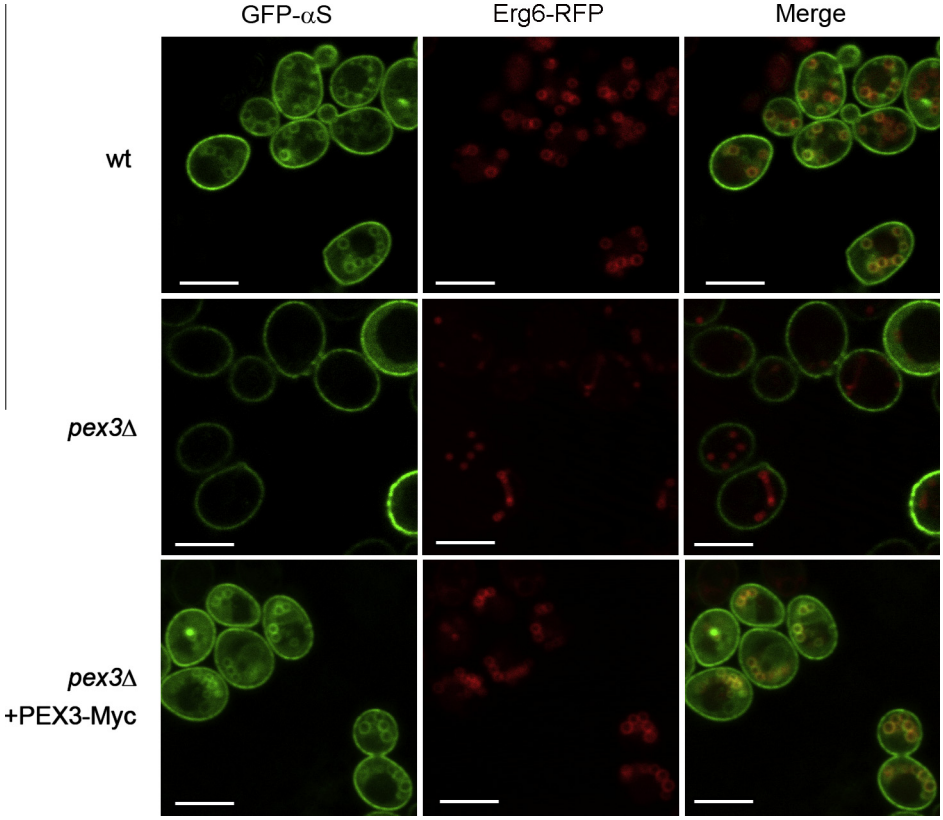

Fig. 1. αS binds to lipid droplets in lipid-loaded, wild-type cells but not in lipid-loaded, *pex3Δ* cells. Strains (wt-3xGFP-αS and *pex3Δ*-3xGFP-αS) were pre-grown in sucrose medium and then shifted into SC-oleate medium for 20 h at 30 °C to induce GFP-αS expression. Cells were imaged by confocal microscopy. To investigate *PEX3* rescue, *pex3Δ*-3xGFP-αS cells were transformed with the plasmid pRS315-PEX3-Myc and then pre-grown and induced like the other strains. Scale bar, 5 μm.

Strain *pex3Δ*-3xGFP-αS, which is otherwise identical to the above strain, had *PEX3* deleted. Cells were grown in liquid media with oleate as the main carbon source and visualized by confocal and fluorescence microscopy.

Fig. 1 (and Fig. S1A) shows wt-3xGFP-αS cells displaying GFP-αS fluorescence around the perimeter of the cell, which is consistent with binding to the plasma membrane, and GFP-αS fluorescence also occurred in multiple circular patterns inside the cells (top left). The same cells were also imaged for lipid droplets, which appear red because Erg6-RFP decorates the surface of the droplets (top middle). The merged image (top right), which shows overlap of the red and green fluorescence, indicates that GFP-αS binds to the lipid droplets in wild-type cells. In contrast, GFP-αS failed to bind to the lipid droplets in identically treated *pex3Δ* cells (*pex3Δ*-3xGFP-αS) (middle panels), which are devoid of peroxisomes (Fig. S2). Strikingly, the binding of GFP-αS to lipid droplets was restored when *PEX3* was added back on a plasmid (bottom panels) (Fig. S1B). The results show that although lipid droplets form in cells devoid of peroxisomes, such lipid droplets, unlike their counterparts in wild-type cells, cannot bind αS.

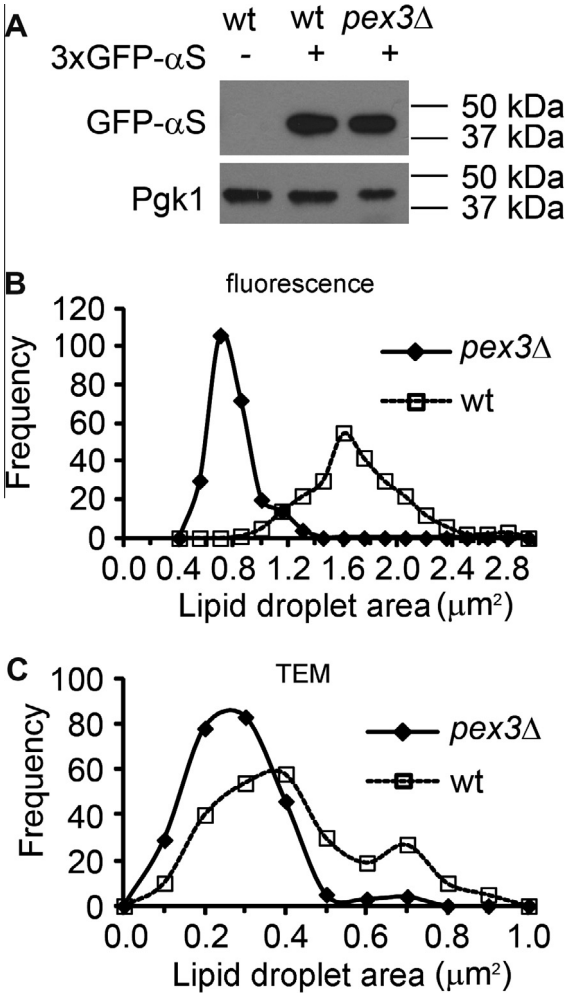

Fig. 2. αS expression and lipid droplet size in lipid-loaded cells. (A) Western blot analysis of wild-type and *pex3Δ* expressing αS. The strains were transformed with the 2μ plasmid pESC-P_{FAA2}-αS, pre-grown in sucrose medium, and then induced for 20 h in SC-oleate. Pgk1 was used as a loading control. (B and C) Plots of frequency *versus* lipid droplet area. The two strains, wt-3xGFP-αS and *pex3Δ*-3xGFP-αS, were induced for 20 h at 30 °C. Fluorescence microscopy was used to estimate diameter (area) (see Fig. S4A), and these results are shown in (B). Transmission electron microscopy was also used to estimate area (see Fig. S4B), and these results are shown in (C). (See Supplementary data for details.).

The variables that govern the binding of αS to lipid droplets are (i) the level of αS expression, (ii) the size of the lipid droplets and (iii) the composition of the lipid droplets. Each of these variables was evaluated in wild-type and *pex3Δ* cells.

3.2. αS expression

Western blot analysis was conducted to ascertain αS expression levels in lysates of wild-type (t-3xGFP-αS) and *pex3Δ* (*pex3Δ*-3xGFP-αS) cells. Because the αS expression levels were similar in the two strains (Fig. 2A), the differences in αS binding to the lipid droplets from the two different strains cannot be due to the level of the αS protein.

3.3. Lipid droplet size and number

Lipid droplet size was estimated using fluorescence microscopy and transmission electron microscopy (TEM) (Fig. 2B and C; Fig. S3). For the fluorescence measurements, lipid droplets in wild-type and *pex3Δ* cells were detected using strains expressing Erg6-RFP, and the diameters of the droplets from multiple cells were measured. The resultant frequency *versus* area plot shows differences with respect to both lipid droplet size and number between the two strains (Fig. 2B). The lipid droplets in *pex3Δ* cells were on average smaller (by ~50%) than the droplets in wild-type cells. For the TEM measurements, the areas of the lipid droplets from multiple cells of each strain were measured using Image J software. The resultant frequency *versus* area plot also shows differences with respect to both lipid droplet size and number between the two strains (Fig. 2C). In this case, the lipid droplets in *pex3Δ* cells were on average smaller (by ~25%) than the droplets in wild-type cells. Although the fluorescence technique gave larger lipid droplet sizes than TEM, both techniques revealed that lipid droplets in *pex3Δ* cells are smaller (by ~25–50%) than the droplets in wild-type cells. Given the known propensity of αS to bind to vesicles of high curvature, one might expect that lipid droplets from *pex3Δ* cells, which have smaller diameters and hence higher curvature than lipid droplets from wild-type cells, would bind αS better than droplets from wild-type cells. But this was not the case.

Using TEM, we also determined that there were on average fewer lipid droplets in *pex3Δ* cells (3.8 ± 0.1/cell) than in wild-type cells (5.4 ± 0.1/cell). This difference in lipid droplet number between the two strains was statistically significant ($p = 6.3 \times 10^{-5}$, student's *t* test; 417 lipid droplets counted in 110 *pex3Δ* cells and 649 lipid droplets counted in 121 wild-type cells).

3.4. Lipid droplet composition

To probe the composition of lipid droplets, we isolated lipid droplets, separated the phospholipids from the neutral lipids, and performed mass spectrometry to identify the components. Phospholipids [PC, PE, phosphatidylinositol (PI) and phosphatidylserine (PS)] and neutral lipids [Stes and TAGs] were analyzed. The major findings were: (i) *Phospholipid monolayer:* The monolayer is predominantly composed of the phospholipids PC and PE for the lipid droplets from both strains (Fig. 3A). (ii) *Shortened acyl chains in phospholipid monolayer:* Lipid droplets from *pex3Δ* cells had a smaller percentage of both 36-carbon (C_{18}/C_{18} at *sn*-1/2 positions) phospholipids (see Fig. 3B and C, Fig. S4 A and B) and 54-carbon ($C_{18}/C_{18}/C_{18}$) TAGs than the droplets from wild-type cells (Fig. S4C). In parallel, lipid droplets from *pex3Δ* cells had a larger percentage of both 32-carbon (C_{16}/C_{16} at *sn*-1/2 positions) phospholipids and 50-carbon ($C_{16}/C_{16}/C_{18}$, *sn* position on glycerol not defined) TAGs than the droplets from wild-type cells (Fig. 3B and C; Fig. S4 A–C). (iii) *Steryl esters:* lipid droplets from *pex3Δ* and

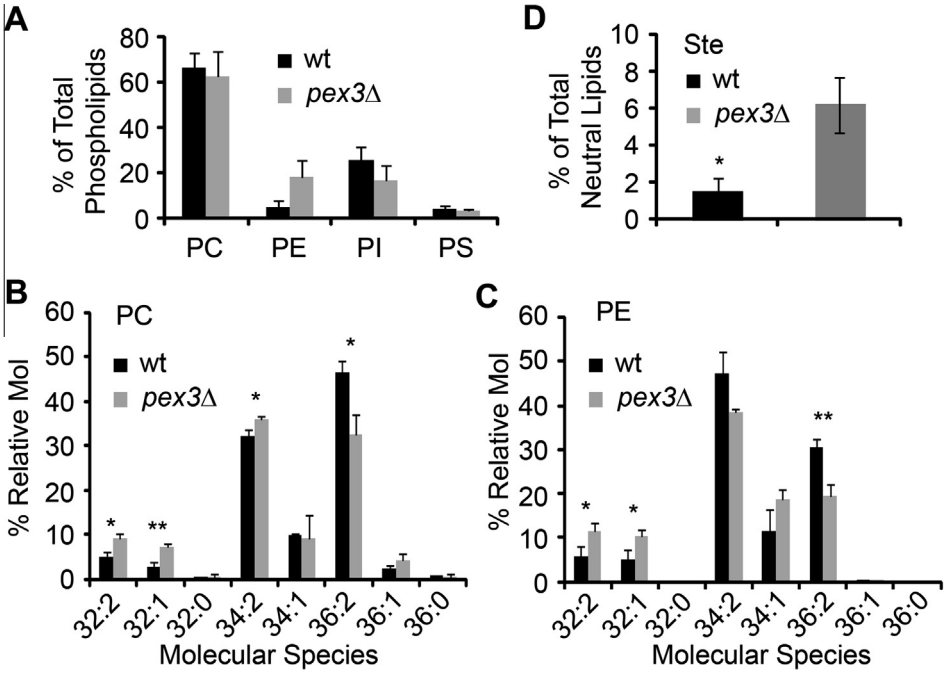

Fig. 3. Identification and quantitation of molecular species in lipid droplets isolated from wild-type and *pex3Δ* cells. (A) The phospholipid content of lipid droplets. (B and C) Analysis of PC and PE molecular species. (D) Steryl esters (Ste). Plot shows the percent of steryl esters in terms of total neutral lipids.*P-values ($p < 0.05$, **$p < 0.01$) were determined using a student's t test ($N = 3$).

wild-type cells had 6% and 2% steryl esters in total neutral lipids, respectively (Fig. 3D).

A mix of electrostatic and hydrophobic interactions governs the binding of αS to biological membranes. The positively charged lysine residues of αS are attracted to negatively charged phospholipid head groups, and the hydrophobic side chains of αS intercalate into the membrane and are attracted to the hydrophobic acyl chains [22]. These two modes of binding enable αS to bind to vesicles composed of either negatively charged phospholipids or zwitterionic phospholipids like PC and PE [23]. Two groups have shown that the strength of the binding of αS to neutral, small unilamellar vesicles correlates with the hydrophobicity (length) of the acyl chains [22,23]. We propose that the shift to the shorter and hence less hydrophobic C_{16} acyl chains contributes to the reduced binding of αS to the lipid droplets in *pex3Δ* cells.

We have shown that a relatively small change in the hydrophobicity of a lipid surface can influence the binding of αS, and the biological significance of this finding is as follows. If the function of αS is linked to its ability to bind membranes and vesicles (as is generally thought), then the failure to bind to these structures, perhaps due to age-related changes in the phospholipid acyl chain hydrophobicity (chain length or saturation), could result in a loss of αS function and consequent neurodegeneration.

Acknowledgments

Support for this work was in part through grants from the National Institute of Neurological Disorders and Stroke (R01NS057656 to SNW) and the United States Department of Energy, Office of Science, Division of Biological and Environmental Research for the lipidomic analysis (DE-FG02-09ER64812 to KDC).

Appendix A. Supplementary data

Supplementary data associated with this article can be found, in the online version, at http://dx.doi.org/10.1016/j.bbrc.2013.07.100.

References

[1] D.J. Moore, A.B. West, V.L. Dawson, T.M. Dawson, Molecular pathophysiology of Parkinson's disease, Annu. Rev. Neurosci. 28 (2005) 57–87.
[2] E.A. Waxman, B.I. Giasson, Molecular mechanisms of alpha-synuclein neurodegeneration, Biochim. Biophys. Acta 1792 (2009) 616–624.
[3] J. Burre, M. Sharma, T. Tsetsenis, V. Buchman, M.R. Etherton, T.C. Sudhof, Alpha-synuclein promotes SNARE-complex assembly in vivo and in vitro, Science 329 (2010) 1663–1667.
[4] A.B. Singleton, M. Farrer, J. Johnson, et al., Alpha-synuclein locus triplication causes Parkinson's disease, Science 302 (2003) 841.
[5] K. Beyer, A. Ariza, Alpha-synuclein posttranslational modification and alternative splicing as a trigger for neurodegeneration, Mol. Neurobiol. 47 (2013) 509–524.
[6] M.H. Polymeropoulos, C. Lavedan, E. Leroy, et al., Mutation in the alpha-synuclein gene identified in families with Parkinson's disease, Science 276 (1997) 2045–2047.
[7] R. Kruger, W. Kuhn, T. Muller, et al., Ala30Pro mutation in the gene encoding alpha-synuclein in Parkinson's disease, Nat. Genet. 18 (1998) 106–108.
[8] J.J. Zarranz, J. Alegre, J.C. Gomez-Esteban, et al., The new mutation, E46K, of alpha-synuclein causes Parkinson and Lewy body dementia, Ann. Neurol. 55 (2004) 164–173.
[9] K.C. Luk, V. Kehm, J. Carroll, B. Zhang, P. O'Brien, J.Q. Trojanowski, V.M. Lee, Pathological alpha-synuclein transmission initiates Parkinson-like neurodegeneration in nontransgenic mice, Science 338 (2012) 949–953.
[10] P.J. McLean, H. Kawamata, S. Ribich, B.T. Hyman, Membrane association and protein conformation of alpha-synuclein in intact neurons. Effect of Parkinson's disease-linked mutations, J. Biol. Chem. 275 (2000) 8812–8816.
[11] N.B. Cole, D.D. Murphy, T. Grider, S. Rueter, D. Brasaemle, R.L. Nussbaum, Lipid droplet binding and oligomerization properties of the Parkinson's disease protein alpha-synuclein, J. Biol. Chem. 277 (2002) 6344–6352.
[12] W.S. Davidson, A. Jonas, D.F. Clayton, J.M. George, Stabilization of alpha-synuclein secondary structure upon binding to synthetic membranes, J. Biol. Chem. 273 (1998) 9443–9449.
[13] B. Nuscher, F. Kamp, T. Mehnert, S. Odoy, C. Haass, P.J. Kahle, K. Beyer, Alpha-synuclein has a high affinity for packing defects in a bilayer membrane: a thermodynamics study, J. Biol. Chem. 279 (2004) 21966–21975.
[14] M.B. Jensen, V.K. Bhatia, C.C. Jao, J.E. Rasmussen, S.L. Pedersen, K.J. Jensen, R. Langen, D. Stamou, Membrane curvature sensing by amphipathic helices: a single liposome study using alpha-synuclein and annexin B12, J. Biol. Chem. 286 (2011) 42603–42614.
[15] Y. Fujiki, Y. Yagita, T. Matsuzaki, Peroxisome biogenesis disorders: molecular basis for impaired peroxisomal membrane assembly: in metabolic functions and biogenesis of peroxisomes in health and disease, Biochim. Biophys. Acta 2012 (1822) 1337–1342.

[16] K. Athenstaedt, P. Jolivet, C. Boulard, M. Zivy, L. Negroni, J.M. Nicaud, T. Chardot, Lipid particle composition of the yeast Yarrowia lipolytica depends on the carbon source, Proteomics 6 (2006) 1450–1459.
[17] S.W. Wanjie, R. Welti, R.A. Moreau, K.D. Chapman, Identification and quantification of glycerolipids in cotton fibers: reconciliation with metabolic pathway predictions from DNA databases, Lipids 40 (2005) 773–785.
[18] R. Bartz, W.H. Li, B. Venables, et al., Lipidomics reveals that adiposomes store ether lipids and mediate phospholipid traffic, J. Lipid Res. 48 (2007) 837–847.
[19] T.R. Flower, C. Clark-Dixon, C. Metoyer, H. Yang, R. Shi, Z. Zhang, S.N. Witt, YGR198w (YPP1) targets A30P alpha-synuclein to the vacuole for degradation, J. Cell Biol. 177 (2007) 1091–1104.
[20] S. Wang, B. Xu, L.C. Liou, Q. Ren, S. Huang, Y. Luo, Z. Zhang, S.N. Witt, Alpha-synuclein disrupts stress signaling by inhibiting polo-like kinase Cdc5/Plk2, Proc. Natl. Acad. Sci. USA 109 (2012) 16119–16124.
[21] D. Binns, T. Januszewski, Y. Chen, et al., An intimate collaboration between peroxisomes and lipid bodies, J. Cell Biol. 173 (2006) 719–731.
[22] V.V. Shvadchak, L.J. Falomir-Lockhart, D.A. Yushchenko, T.M. Jovin, Specificity and kinetics of alpha-synuclein binding to model membranes determined with fluorescent excited state intramolecular proton transfer (ESIPT) probe, J. Biol. Chem. 286 (2011) 13023–13032.
[23] G.F. Wang, C. Li, G.J. Pielak, 19F NMR studies of alpha-synuclein–membrane interactions, Protein Sci. 19 (2010) 1686–1691.